



Removal of tetracycline from aqueous solutions using polyvinylpyrrolidone (PVP-K30) modified nanoscale zero valent iron

Hua Chen^{a,b}, Hanjin Luo^{a,b,c,*}, Yuecun Lan^{a,c}, Tingting Dong^{a,b}, Bingjie Hu^{a,b}, Yiping Wang^{a,c}

^a College of Environmental Science and Engineering, South China University of Technology, Guangzhou 510006, Guangdong, China

^b The Key Laboratory of Pollution Control and Ecosystem Restoration in Industry Clusters of Ministry of Education, Guangzhou 510006, Guangdong, China

^c The Key Laboratory of Environmental Protection and Eco-Remediation of Guangdong Regular Higher Education Institutions, Guangzhou 510006 China

ARTICLE INFO

Article history:

Received 28 January 2011

Received in revised form 25 March 2011

Accepted 20 April 2011

Available online 27 April 2011

Keywords:

Antibiotics

Zero-valent iron nanoparticles

Tetracycline (TC)

Mechanisms

LC-MS

ABSTRACT

The interactions of tetracycline (TC) with nanoscale zerovalent iron (NZVI) modified by polyvinylpyrrolidone (PVP-K30) were investigated using batch experiments as a function of reactant concentration, pH, temperature, and competitive anions. Transmission electron micrographs (TEM), BET surface area and Zeta (ζ)-potential analyses indicated that the mean particle size was 10–40 nm with a surface area of 36.90 m²/g, and a iso-electric point of PVP-NZVI was 7.2. The results of X-ray diffraction (XRD) and high-resolution X-ray photoelectron spectroscopy (HR-XPS) of modified nanoscale zerovalent iron (PVP-NZVI) revealed that the iron nanoparticles likely have a core of zero-valent iron (Fe⁰), while a shell is largely made of iron oxides. Degradation of TC was strongly dependent on pH and temperature. The presence of silicate and phosphate strongly inhibited the removal of TC, whereas acetate and sulfate only caused slight inhibition. LC-MS analysis of the treated solution showed that the degradation products from TC resulted from the removal of functional groups from the TC ring. The degradation products were detected both in the treated solution (initial pH of 3.0 and 6.5) and on the surface of PVP-NZVI after 4-h interaction, indicating that PVP-NZVI can adsorb both TC and its degradation products.

Crown Copyright © 2011 Published by Elsevier B.V. All rights reserved.

1. Introduction

Tetracyclines (TCs), including oxytetracycline (OTC), tetracycline (TC), and chlortetracycline (CTC), are a group of broad-spectrum antibiotics applied to livestock as additives to combat diseases. In natural soils, the sorption and transport behaviors of these chemicals are similar despite their structural variances [1]. In China, the use of veterinary antibiotics in animal feeds has been regulated since 1989 and only prophalactic antibiotics such as monensin, salinomycin, destomycin, bacitracin are permitted as feed additives. However, TCs used for therapeutic purpose, are often illegally used as feed additives by some farming operations [2]. Over 8000 t of antibiotics are utilized as feed additives each year [3]. Zhang [4] reported the main chemistry ingredients of livestock and poultry manures of typical intensive feeding in Chinese seven provinces and found that the average contents of terramycin, tetracycline and aureomycin were 9.09 mg/kg, 5.22 mg/kg, 3.57 mg/kg, the variational range of each antibiotics were 1.05–134.75 mg/kg, 0–78.57 mg/kg, 0–78.57 mg/kg, respectively. A survey of the

occurrence of TCs in sandy soils fertilized with liquid manure was conducted in northwestern Germany. At least three of the 14 agricultural fields surveyed had higher concentrations than the trigger value (100 µg/kg) of European Agency for the Evaluation of Medicinal Products for TCs [5]. In the United States, the annual consumption of TCs in swine and poultry husbandry reached 2.3 and 0.63 million kilograms, respectively, in the late 1990s [6]. Most antibiotics enter the environment through municipal effluents, sewage sludge, solid waste, and manure applications. Recent studies have reported detection of TCs at around 0.15 µg/L in groundwater and surface water [7], 86–199 µg/kg in soil, 4.0 mg/kg in liquid manure [8], and 3 µg/L in farm lagoons [9]. De Liguoro et al. [10] reported that OTC can persist in composting manure for at least five months. Consequently, there have been increasing concerns that the wide application of antibiotics in livestock production will promote the evolution of microbial populations resistant to the antibiotics used by humans. Even low concentrations of pharmaceuticals released from the environmental matrix into water can pose serious environmental damages. Thus, it is of great importance to develop some efficient and cost-effective treatment technologies to remove such compounds.

It has been suggested that highly reactive nanoscale zero valent iron (NZVI) can be applied in groundwater remediation and other environmental applications. For example, NZVI can effectively transform many environmental contaminants including

* Corresponding author at: College of Environmental Science and Engineering, South China University of Technology, Guangzhou 510006, Guangdong, China.
Tel.: +86 20 3938 0537; fax: +86 20 8711 0517.

E-mail address: luohj@scut.edu.cn (H. Luo).

chlorinated solvents, organochlorine pesticides, polychlorinated biphenyls, organic dyes, and inorganic pollutants [11–19]. One of the reasons for the high reactivity of NZVI is that it possesses large specific surface area which provides more active sites for the degradation of contaminants. It is recognized that NZVI tends to aggregate rapidly due to van der Waals and magnetic forces, making it difficult for NZVI to interact with target contaminants [11]. To prevent aggregation of NZVI, particle stabilization has been commonly practiced by attaching a stabilizer such as a soluble polymer or surfactant onto the nanoparticles [20]. Sun et al. [16] demonstrated that polyvinyl alcohol-co-vinylacetate-co-itaconic acid (PV3A) could serve as an effective dispersant of NZVI. He and Zhao [11,21] employed a food-grade starch and sodium carboxymethyl cellulose (CMC) as preagglomeration stabilizers to obtain highly dispersed ZVI nanoparticles. Polyvinylpyrrolidone (PVP-K30) is water-soluble, low-cost, environmentally friendly and commonly used in food processing. Recently, PVP-K30 has been successfully used as the capping molecules to synthesize highly monodisperse wurtzite ZnO nanoparticles and the sterically stabilized PVP-silver nanoparticles (PVP-AgNPs) [22,23]. Therefore, the present study evaluated the using of PVP-K30 as a stabilizer for preparing physically more stable and chemically more reactive NZVI for the removal of TC in water. Removal of TC from the aqueous phase has been widely studied using materials such as aluminum and iron hydrous oxides, clay minerals, palygorskite, activated carbon, multiwalled carbon nanotubes, hydrous manganese oxide and with various degrees of success [1,24–28]. However, almost no attention has been paid to the interaction of TC with NZVI.

In the present study, PVP-K30 was evaluated for its efficacy as a NZVI dispersant. The objectives of the present work were to investigate the interaction of tetracycline with PVP-K30 modified NZVI (PVP-NZVI) and to derive the removal parameters applicable over a wide range of conditions, such as pH, temperature, reactant concentration, type of competitive anion, and reaction time. Finally, mass spectrometry (MS) was used to obtain the structural information of TC degradation products and the removal mechanisms were also investigated.

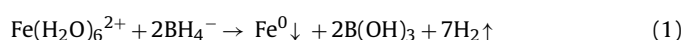
2. Experimental

2.1. Materials and chemicals

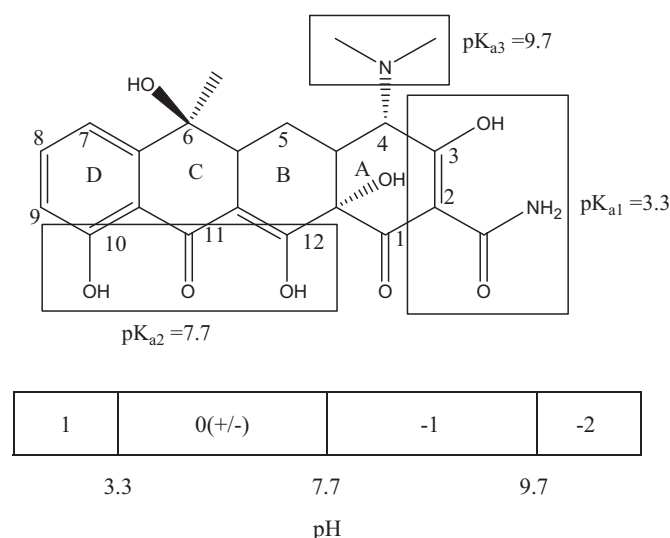
Hydrochloride salt of tetracycline (TC, $\geq 95\%$ purity, MW: 480.90) was purchased from Sigma Co. and the structure of TC was showed in Fig. 1. Polyvinylpyrrolidone (PVP-K30, MW: 58000) was purchased from Aladdin-reagent Co., China. Na_2SO_4 , NaH_2PO_4 , NaOH , HCl , KBH_4 , NaCl , and other reagents were of analytical grade and were purchased from Guangzhou Chemical Reagent Factory. All chemicals were used as received without further purification. All solutions were prepared with deionized water (18 M Ω Milli-Q) and stored at 4 °C.

2.2. Synthesis procedures

The PVP-NZVI particles were synthesized by using the well-known liquid-phase reduction method [29] based on the following reaction:



The preparation was carried out in a 500-mL flask attached to a vacuum pump. First, 0.02 mol $\text{FeSO}_4 \cdot 7\text{H}_2\text{O}$ was dissolved into 100 mL ethanol solution (30% volume), then PVP-K30 powder (the weight ratio of PVP to NZVI is 0.35–1) was added with vigorous agitation. After sparging with N_2 for 15 min, 100 mL 0.01 M borohydride solution was slowly added into the above mixture and stirred for 20 min at 25 °C. Fe^{2+} was reduced by BH_4^- to form black NZVI



Note: the vertical bars correspond to the pH at which equimolar concentrations of adjacent species are present.

Fig. 1. Structure of tetracycline (TC) and the pH-dependent speciation of tetracycline (TC) [47].

particles immediately. NZVI particles were collected by vacuum filtration and washed several times with deionized (DI) water and ethanol. The resulting black solids were vacuum-dried for 10 h at 40 °C, broken up by a spatula and stored in a N_2 -purged desiccator.

Preparation of bare-NZVI, without adding PVP-K30, the remaining steps was the same as the preparation method of PVP-NZVI.

Procedure of preparation of hydrous oxide of Fe (HFO) was given in detail in study of Gu and Karthikeyan [24].

2.3. Methods

2.3.1. TEM (transmission electron microscope)

TEM images were obtained using a JEOL (Japan) JEM-100CX-II transmission electron microscope (TEM) operated at accelerating voltage 100 kV. The freshly prepared PVP-NZVI and bare-NZVI samples were dispersed by ultrasonic before test.

2.3.2. HR-XPS (high-resolution X-ray photoelectron spectrometer)

Surface composition to a depth of <5 nm of the nanoparticles was analyzed with a AXIS Ultra DLD HR-XPS (Kratos, England). All samples were dried in vacuum at room temperature and then sealed under nitrogen gas to avoid sample oxidation before analysis.

2.3.3. BET surface area

PVP-NZVI samples were pre-dried at 40 °C in a vacuum desiccator. The samples were then outgassed for 12 h at 200 °C under vacuum. Surface area of NZVI particles was determined from the corresponding N_2 adsorption/desorption isotherms obtained at 77 K with an automatic instrument (NAVO 2200, Quantachrome Instrument, FL, USA).

2.3.4. X-ray diffraction (XRD)

X-ray diffraction patterns were collected using a Bruke D8-advance X-ray diffractometer at 40 kV and 40 mA. A $\text{Cu K}\alpha$ radiation source was used in the X-ray tests. Iron nanoparticles were scanned from 10° to 60°, the scanning rate was set at 0.020°/step and 17.7 s/step.

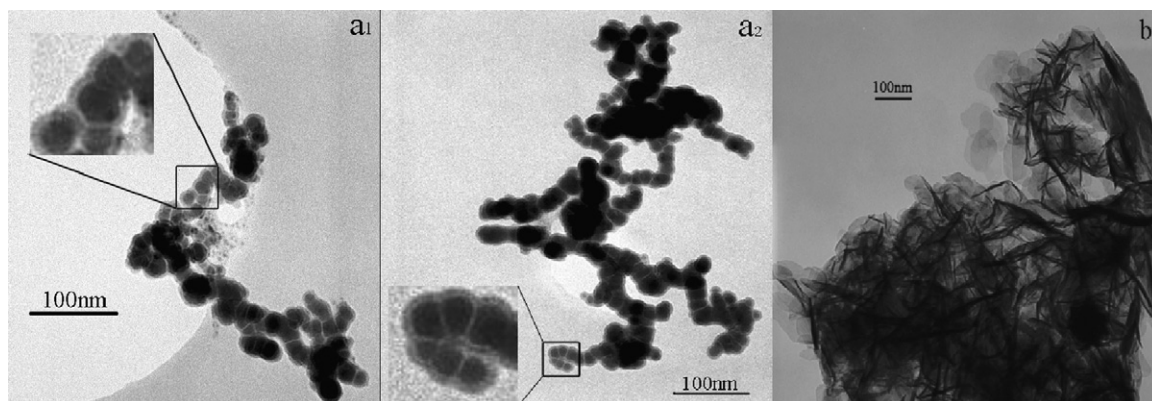


Fig. 2. (a₁, a₂) TEM images of the synthesized PVP-NZVI particles. The inset in the figures showed the core-shell structure of PVP-NZVI. (b) TEM image of the synthesized bare-NZVI particles (the iron nanoparticles in the absence of PVP-K30).

2.3.5. Iso-electric point (IEP)

Zeta (ζ)-potential as a function of the solution pH was used to determine the iso-electric point of PVP-NZVI and bare-NZVI. The solution pH was adjusted with 0.01 M NaOH or 0.01 M HCl. During the experiment, the system was operated under an inert atmosphere. The fresh prepared iron nanoparticle slurry (0.5 g/L) was shaken for 20 min at 150 rpm until a stable ζ potential was reached. Then samples were collected with glass syringes, and analyzed by Nano-ZS90 (Malvern, United Kingdom).

2.3.6. Analysis of TC

The concentration of TC in the solution was analyzed using High Performance Liquid Chromatography (Shimadzu, Japan). Column: Agilent HC-C18, 5 μ m, 4.6 mm \times 250 mm; The mobile phase was a mixture of 0.01 M oxalic acid-acetonitrile-methanol (45:35:20, v/v); flow rate: 1.0 mL/min; detector: UV at 360 nm and sample size: 20 μ L [24,30]. The correlation coefficient of the standard curve ($n=6$) was greater than 0.998. TC recoveries in controls (no PVP-NZVI), determined by HPLC, were >95% at pH between 4.0 and 9.5.

2.3.7. HPLC/ESI-MS measurements

HPLC/ESI-MS measurements were carried out using a HCT-Plus ion-trap mass spectrometer (Bruker-Daltonics, Bremen, Germany) equipped with a HPLC system (Agilent 1100 series, autosampler, gradient pump and degasser, Agilent Technologies, Germany) and a Zorbax Extend-C18 100 mm \times 2.1 mm column with 3.5- μ m particle size (Agilent Technologies, Germany). The mobile phase was a mixture of 0.01 M formic acid-acetonitrile-methanol (45:35:20, v/v) in an isocratic system at a flow rate of 0.2 mL/min. The mass spectrometer was run in negative ion mode. They were used to determine the products in supernatant samples after 4-h' interaction with PVP-NZVI (initial pH of 3.0 and 6.5) and the dissolved sample (the centrifuged PVP-NZVI which was dissolved with concentrated hydrochloric acid and then diluted by deionized water). All the samples determined by LC-MS were adjusted to pH = 6.5 by 0.1 M NaOH and 0.1 M HCl.

2.3.8. Total organic carbon (TOC) analysis

TOC was determined with a total organic carbon analyzer (Model TOC-VCPN, Shimadzu, Kyoto, Japan), which utilizes oxidative combustion followed by infrared detection.

2.4. Batch experiments

In the batch experiments, TC solutions (C_{TC} 0.225 mM; ionic strength 0.01 M NaCl) were prepared fresh daily for each batch test. To start the experiments, 25 mL of the prepared TC solution was

purged with nitrogen for 10 min in a 50 mL beaker. Then the solution was mixed with 0.0025 g freshly prepared NZVI. The beaker sealed with aluminum foil was continuously shaken (150 rpm) for 0.33, 0.5, 1, 2, 3, 4, 6 h at 25 °C. Parallel experiments were conducted without nanoparticles (blank). At selected time intervals, pairs of centrifuge tubes were centrifuged (8700 \times g for 5 min) and then collected with glass syringes and filtered through a 0.45 μ m membrane filter for analysis. One or two drops of 12 mol/L HCl were added into the filtrate to adjust solution pH to 1–2 in order to dissociate the complex of TC and Fe in solution. After 2 h, the Fe concentration in the filtrate was determined by the Z-2000 atomic absorption spectrophotometer (AAS Hitachi Corp., Japan). Each experiment, including blanks, was run in duplicate. The pH of the samples was measured by a pH electrode. Other experimental conditions and measurements except the pH reaction were set at the condition of dosage of PVP-NZVI, 0.1 g/L; temperature, 25 °C; pH, 6.5.

Batch tests were performed in Na electrolyte solutions of varying strength and anionic counterions, using solutions of 100 mg/L TC in 0.1, 1, 10, and 100 mM solutions of NaH₂PO₄, Na₂SiO₃, Na₂SO₄, CH₃COONa and NaHCO₃. The pH of the suspension was adjusted at 6.5. After 4 h, the suspension was centrifuged (8700 \times g for 5 min), filtered through a 0.45 μ m membrane filter, and analyzed for TC as described above.

3. Results and discussion

3.1. Characterizations of synthesized NZVI particles

TEM images of PVP-NZVI (Fig. 2a₁ and a₂) show that the PVP-NZVI particles were nearly spherical with a size range of 10–40 nm in diameter and these nanoparticles have a core-shell structure. The shell (1–10 nm) probably resulted from iron oxide or PVP, while the core was attributed to Fe⁰ [31]. In contrast, in the absence of the PVP, freshly prepared bare-NZVI particles appeared as bulkier acerate or dendritic flocs rather than discrete particles due to the aggregation of Fe particles (Fig. 2b). The aggregated structure of Fe particles was attributed to the magnetic forces and van der Waals forces between Fe particles. For the survey of Fe 2p core levels (Fig. 3a), the photoelectron peaks at 710.67 eV, 719.57 eV and 724.43 eV which suggest that the surface of iron nanoparticles consist mainly of the layer of iron oxides [12,32]. Furthermore, a peak at around 706.83 eV can also be observed, suggesting the peak of zero-valent of iron (Fe⁰). Fig. 3b shows a full survey of the surface composition before and after the reaction, the sample of after reaction emerged with the peak at N 1s = 400.3 eV and the increase of intensity of peaks for O and C showing that part of the target contaminant and products in solution had been adsorbed on the surface of nanoparticles.

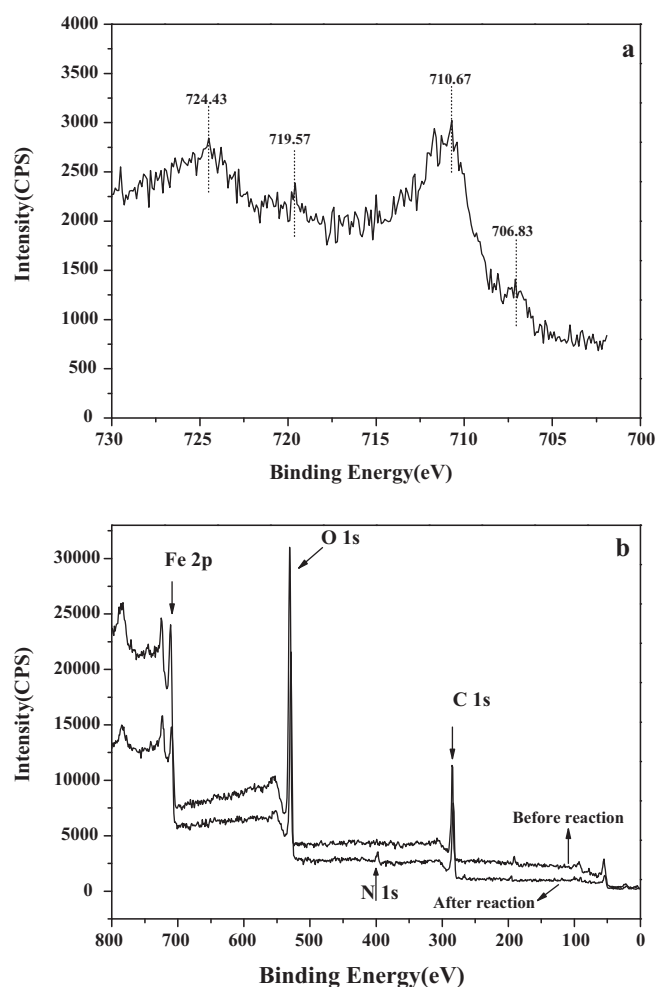


Fig. 3. XPS response of (a) Fe 2p core levels of iron nanoparticles and (b) full survey of before and after reaction.

The BET-measured specific surface area (S_{BET}) of synthesized PVP-NZVI is $36.90 \text{ m}^2/\text{g}$. The effective mean radius of the iron particles is calculated at 10 nm calculated using Eq. (2)

$$r = 3[\rho * S_{\text{BET}}]^{-1} \quad (2)$$

and a density (ρ) for Fe of $7870 \text{ kg}/\text{m}^3$, which is consistent with the TEM results. Furthermore, the XRD pattern of freshly synthesized PVP-NZVI (Fig. 4a) indicated that PVP-NZVI particles mainly appeared in the zero-valent iron state, as demonstrated by the basic reflection at 2-theta 44.9° . XRD peaks at 2-theta 44.9° expected for $\alpha\text{-Fe}^0$ have been reported for these particles [13,14,33]. Since only broad peaks appeared in the XRD spectra of HFO (Fig. 4b), it is confirmed that the hydrous oxides are noncrystalline minerals. The BET-measured specific surface area (S_{BET}) of HFO is $310 \text{ m}^2/\text{g}$ (other characterizations of HFO not shown). The result was in good agreement with the reports of Gu and Karthikeyan [24] and Goldberg and Johnston [34], specific surface area (S_{BET}) of HFO were $322 \text{ m}^2/\text{g}$ and $290 \text{ m}^2/\text{g}$, respectively. Numerous previous studies suggested that the ζ -potential of bare-NZVI was negative only when pH was higher than the isoelectric point (IEP) of 8.1–8.2 [16,17]. However, Fig. 4c reveals that the IEP of PVP-NZVI was about 7.2. Considering the pH-dependent speciation of tetracycline and the isoelectric point of PVP-NZVI, initial solution pH in the experiments was set at 6.5.

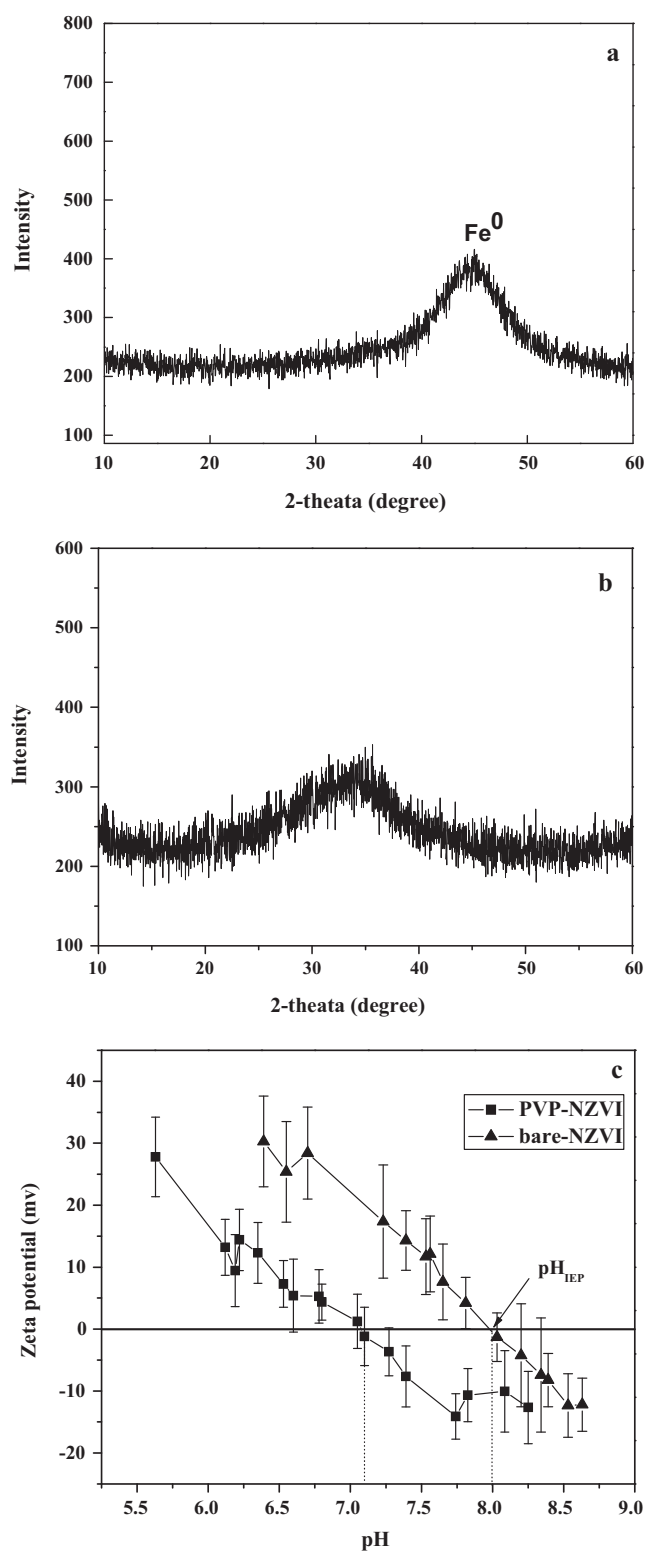


Fig. 4. (a) X-ray diffraction analysis of PVP-NZVI. (b) X-ray diffraction analysis of HFO. (c) Zeta (ζ)-potential of PVP-NZVI and bare-NZVI as a function of solution pH.

3.2. Factors affecting the removal of TC

3.2.1. Dosage of PVP-NZVI

The removal efficiency of TC with reaction time from 10 min up to 6 h under different dosages of NZVI is displayed in Fig. 5. The

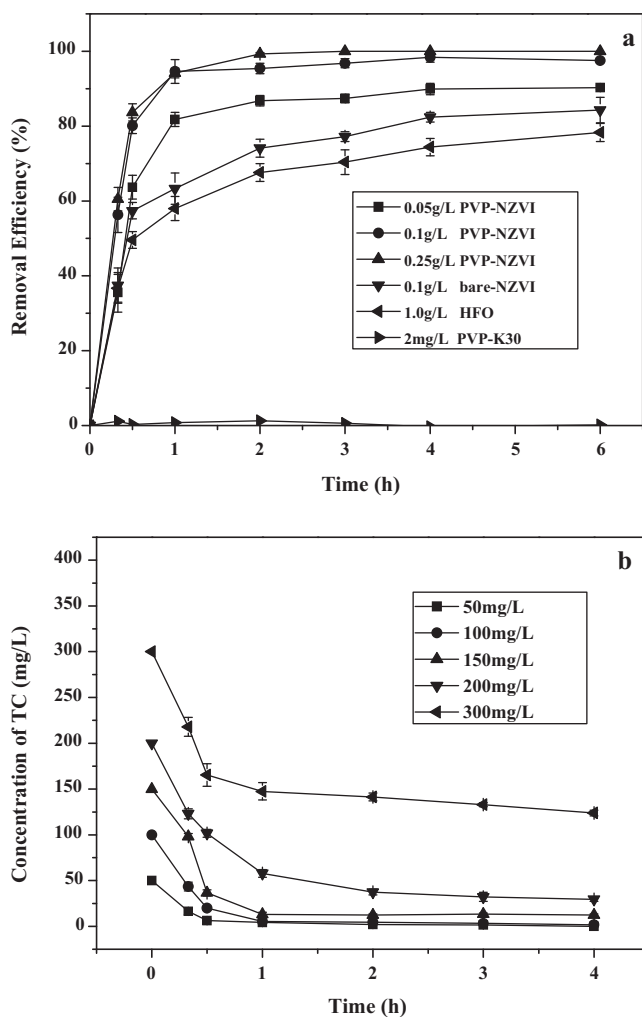


Fig. 5. (a) Removal efficiency of TC by (0.1 g/L, 0.05 g/L, and 0.25 g/L) PVP-NZVI and 0.1 g/L bare-NZVI and 1.0 g/L HFO (initial concentration of TC, 100.0 mg/L; temperature, 25 °C; pH, 6.5). (b) Effect of initial TC concentration on the removal efficiency (dosage of PVP-NZVI, 0.1 g/L; temperature, 25 °C; pH, 6.5).

removal efficiency of TC is defined as

$$\text{Removal efficiency} = \frac{C_0 - C_t}{C_0} \times 100\% \quad (3)$$

where C_0 and C_t represent the concentrations of TC at time 0 and t , respectively. Fig. 5a shows that TC removal efficiency was greatly affected by reaction time. At low dosage (0.05 g/L PVP-NZVI), approximately 90% of TC was removed after 6 h. The removal efficiency of TC increased with increasing PVP-NZVI dosage. As the dosage of PVP-NZVI increased from 0.1 to 0.25 g/L, more than 80% of TC was removed within 30 min and approximately 100% within 4 h. No decrease of TC concentration was observed in the control batch reactor containing 2.0 mg/L PVP-K30; therefore, sorption or partitioning of TC to PVP-K30 was negligible. Fig. 5a shows that 0.05 g/L PVP-NZVI exhibited better removal efficiency than 0.1 g/L bare-NZVI. Less removal of TC by the bare-NZVI could be a result of the aggregation of the particles which indicate that the interactions between the particles and the contaminant are minimal. Only 78.3% of TC was removed by 1.0 g/L HFO after 6 h. The S_{BET} of PVP-NZVI is just about one-tenth of that of HFO, however, the TC removal efficiency of TC by 0.1 g/L PVP-NZVI is much better than that by 1.0 g/L HFO. The reason is that compared with HFO, PVP-NZVI presents not only adsorption but also degradation (detail discuss later).

Table 1
Chemical equations and stability constants of soluble species.

Chemical equation	lg K	Reference
$\text{Fe}^{2+} + \text{OH}^- = \text{Fe}(\text{OH})^+$ (4)	4.5	[36]
$\text{Fe}^{2+} + 2\text{OH}^- = \text{Fe}(\text{OH})_2$ (5)	7.4	
$\text{Fe}^{2+} + 3\text{OH}^- = \text{Fe}(\text{OH})_3^-$ (6)	11	
$\text{Fe}^{2+} + 4\text{OH}^- = \text{Fe}(\text{OH})_4^{2-}$ (7)	10	

3.2.2. TC concentration

The removal of TC using PVP-NZVI as a function of initial TC concentration was examined in the concentration range of 50.0–300.0 mg/L. The amount of TC removed increased with the increase of initial TC concentration, and then reached equilibrium after 2 h (Fig. 5b). The removal of TC occurred immediately at the beginning of reaction because of the abundant reactive sites available on the surface of the fresh material. After 2 h, as most reactive sites have been occupied, TC degradation proceeded with a much slower process. Thus, removal rates and capacity were limited by the lack of reactive sorption sites.

3.2.3. pH

pH is a key factor affecting removal efficiency of TC. TC exhibits three macroscopic acidity constants. In aqueous environment, the first deprotonation ($\text{p}K_1 = 3.3$) occurs at O3; the second $\text{p}K$ value ($\text{p}K_2 = 7.7$) is attributed to O11 and O12; and the third one ($\text{p}K_3 = 9.7$) is ascribed to the protonated nitrogen of the dimethylamino group (Fig. 1) [35]. As a result, TC exists as a cationic, zwitterionic and anionic species under acidic, moderately acidic to neutral and alkaline conditions (Fig. 1), respectively. The removal efficiency of TC was studied as a function of initial pH (3.0, 6.5, 8.0, 10.0) within 4 h (Fig. 6a). At pH 3.0 and pH 6.5, the removal efficiency of TC was approximately 100%, but at pH 8.0 and pH 10.0 it decreased to only 53.5% and 43.1%, respectively. These results indicated that the removal of TC by PVP-NZVI was effective in both acidic and neutral pH.

As the initial pH at 3.0 and 6.5 (Fig. 6b), the removal efficiency of TC was approximately 100% and the final pH reach 5.3 and 6.7, respectively. This can be explained by ionization of both the adsorbate and the adsorbent, which caused repulsion at the surface and sequent decrease of the TC adsorption. All TC species in solution have positive, zwitterion and negative charges as H_3L^+ , H_2L^0 , HL^- and L^{2-} (Fig. 1). In this pH range (3.0 and 6.5), H_2L^0 is the predominant TC species while the NZVI surfaces are positive (pH_{IEP} of PVP-NZVI = 7.2) causing H_2L^0 species of TC was adsorbed onto the positive charged PVP-NZVI surface. When initial pH at 8.0 and 10.0, the removal efficiencies of TC were 53.5% and 43.1%, respectively. As pH is above 7.7 ($\text{p}K_{\text{a}2}$), HL^- and L^{2-} are the predominant TC species while the NZVI surfaces are also negative (pH_{IEP} of PVP-NZVI = 7.2) causing electrostatic repulsion. Consequently, the removal efficiency of TC at pH 8.0 and 10.0 decreased. Although there is a significant electrostatic interaction between TC and PVP-NZVI, a rather strong non-electrostatic interaction also exists. Fig. 6c shows that the concentration of total dissolved iron increased initially, and then decreased slowly after 1 h. Yellow flocculent precipitates were observed at pH 3.0 and 6.5, which were considered as Fe-tetracycline complexes rather than hydroxide precipitation. This was attributed to the fact that the formation constant of Fe-tetracycline complexes (13.4) [35] is higher than that of Fe-OH complexes (Table 1).

3.2.4. Evolution of pH value during the reaction

Fig. 6b shows the variations of pH in various processes. The final pH was much higher than the initial pH except at pH 10.0. The predominant electron receptors were water and dissolved oxygen

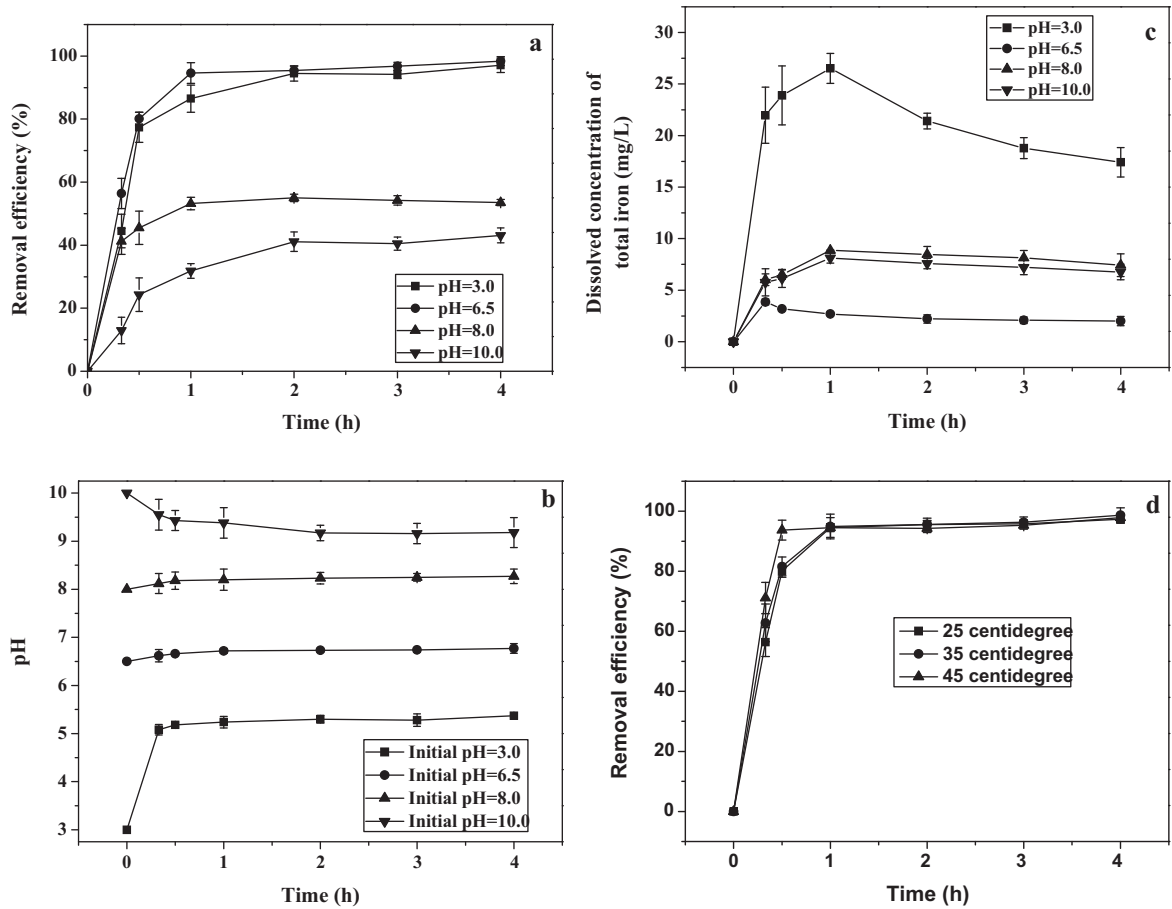
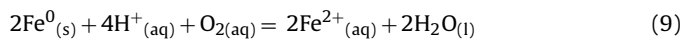
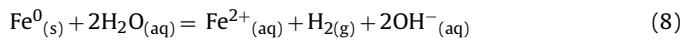


Fig. 6. (a) Influence of pH on the removal of TC by PVP-NZVI. (b) Evolution of pH value during the reaction. (c) Evolution of dissolved concentration of total iron value during the reaction. (d) Influence of initial temperature on the removal of TC by PVP-NZVI.

based on the anaerobic corrosion Eq. (8) and aerobic corrosion Eq. (9), respectively.



According to the above reactions, these NZVI particles redox should produce a characteristic increase in solution pH [13,37]. Fig. 6c shows that pH increased with time and then reached equilibrium. Lower pH promoted the corrosion rate leading to the release of OH^- . Parallel experiments in which initial pH was settled at 10.0 were conducted without nanoparticles. The results revealed that both the TC concentration and the pH decreased. This observation was in agreement with the findings reported by Rubert and Pedersen [38].

3.2.5. Temperature

The effect of temperature on the removal of TC was investigated. The solutions were incubated at different temperatures (25 °C, 35 °C and 45 °C) for 10 min before reactions. Fig. 6d showed that as the temperature increased from 25 °C to 45 °C, the removal efficiency of TC increased from 56.4% to 71.1% within initial 10 min. The experiments (25 °C, 35 °C and 45 °C) reached equilibrium within 4 h and the removal rate of TC at 45 °C was much faster than that obtained at other temperatures. It could be the mobility of TC from solution to nanoparticles increased at higher temperature and higher temperature also accelerated iron corrosion.

3.2.6. TOC

The curves of TOC of filtrate as a function of reaction time at different initial pH are shown in Fig. 7. TC was almost completely removed after 4 h at pH 3.0 and 6.5. The removal efficiency of TOC was consistent with the removal efficiency of TC at different pH (Fig. 6a). If all TC in solution are transformed by PVP-NZVI without the absorption, TOC should be constant over the reaction time and the concentration of TC should decrease. However, as shown in Fig. 7, both TC and TOC decreased with the increasing time. This might be resulted from the sorption and complex formation

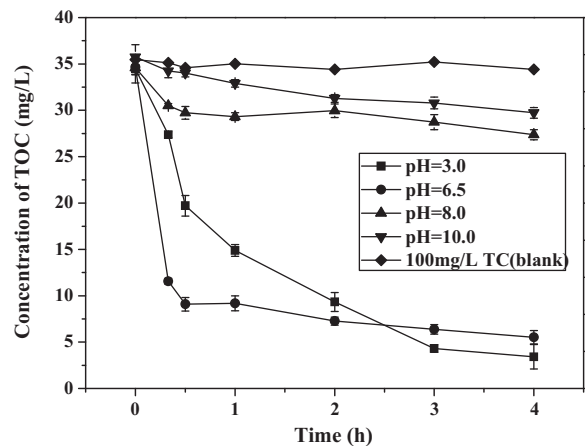


Fig. 7. Variation of the TOC values determined during the reaction between TC and PVP-NZVI at different initial pH.

Table 2
Percent removal rate of TC removal in the presence of competitive anions.

Anions, mM	Percentage removal of TC in the presence of anions				
	SO ₄ ²⁻	HCO ₃ ⁻	H ₂ PO ₄ ⁻	CH ₃ COO ⁻	SiO ₃ ²⁻
0	98.4	98.4	98.4	98.4	98.4
0.1	98.4	98.4	98.4	98.4	98.4
1	98.4	97.1	82	98.4	87.6
10	97.8	94.5	71.3	98.4	85.2
100	96.2	91.6	60.2	97.9	84.8

^aInitial TC: 100.0 mg/L; PVP-NZVI: 0.1 g/L in 0.01 M NaCl, pH 6.5, at 25 °C.

^bNote: % removal of TC in the presence of anions: *n* = 3, average of triplicate results where the standard deviation is less than 10%.

with PVP-NZVI. The overall TC disappearance in such batch systems therefore includes not only reduction reaction but also losses due to sorption. This phenomenon was also found in the work of Burris et al. [39]. They have carefully differentiated sorption from reaction.

3.2.7. Competitive anions

The effect of competitive anions (SO₄²⁻, HCO₃⁻, H₂PO₄⁻, CH₃COO⁻, SiO₃²⁻) on the removal of TC by PVP-NZVI was shown in Table 2. Competitive anion concentrations up to 100 mM caused

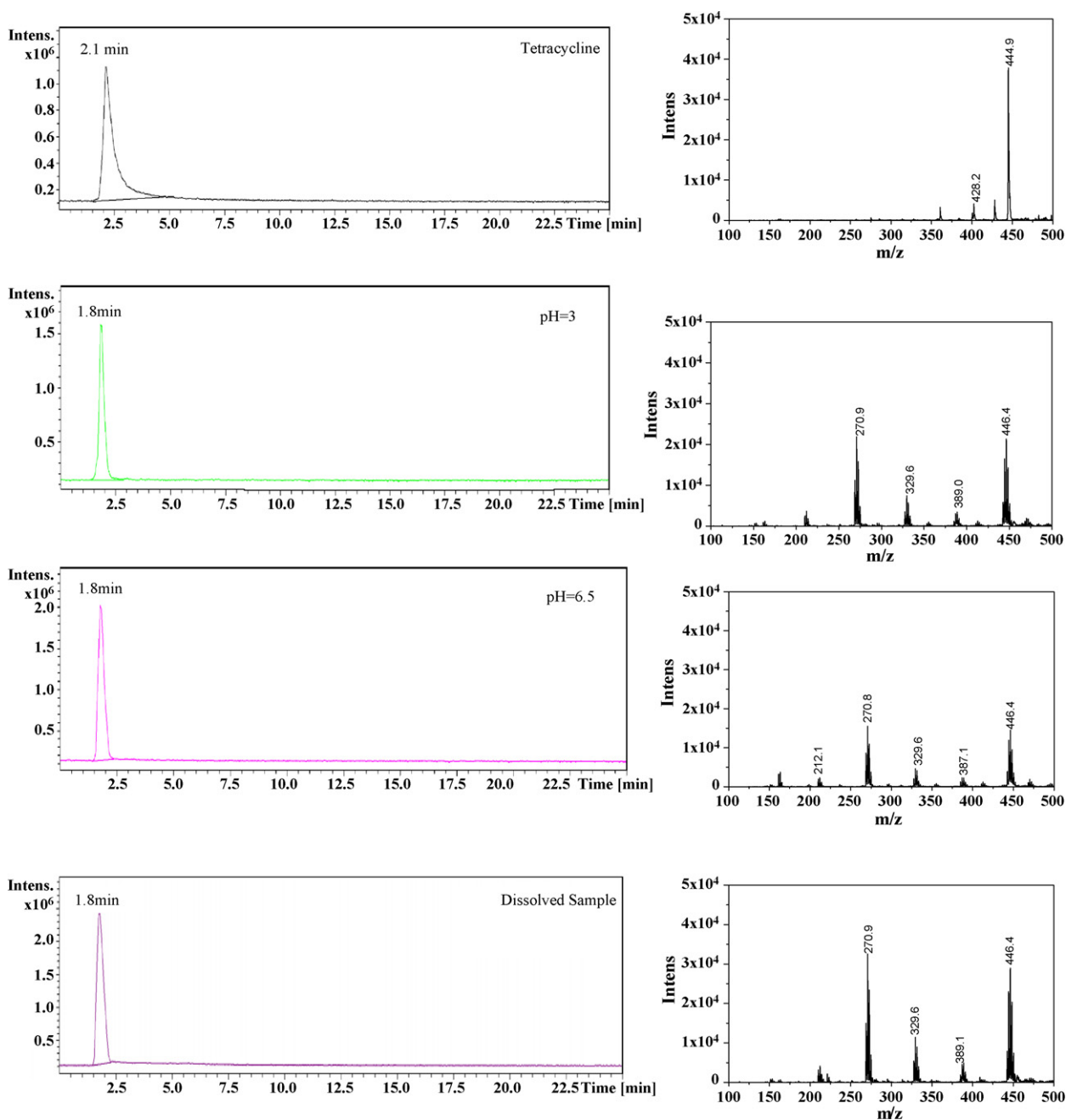
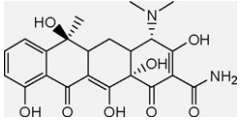
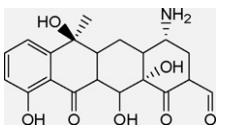
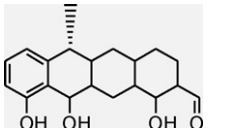
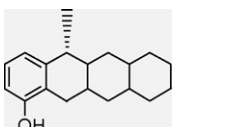


Fig. 8. LC-MS spectra of TC, supernatant samples (initial pH 3.0 and 6.5) and the dissolved sample. The insets show the mass spectra eluted at 2.1 and 1.8 min.

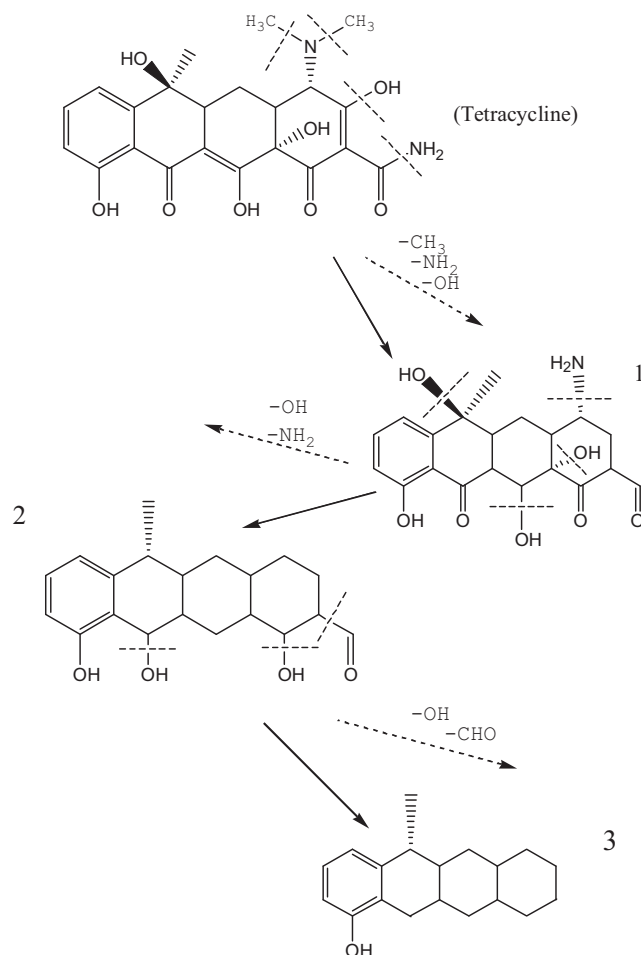
Table 3
Degradation products of TC by PVP-NZVI.

Compound	<i>m/z</i>	Molecular weight	Formula	Possible structure
Tetracycline	444.9	444.4	C ₂₂ H ₂₄ N ₂ O ₈	
Product 1	387.1	389.4	C ₂₀ H ₂₃ NO ₇	
Product 2	329.6	330.4	C ₂₀ H ₂₆ O ₄	
Product 3	270.8	270.2	C ₁₉ H ₂₆ O	

the removal efficiency of TC to decrease from 98.4% to 97.9%, 96.2%, and 91.6% for CH₃COO⁻, SO₄²⁻ and HCO₃⁻ ions, respectively. The addition of 100 mM SiO₃²⁻ and H₂PO₄⁻ reduced the removal of TC to 84.8% and 60.2%, respectively. The reason for the negative effect of H₂PO₄⁻ was that phosphate was a inner-sphere complex-forming anion which was strongly sorbed to mineral surfaces, thus decreasing the sorption of TC on PVP-NZVI [37,40]. Others found that H₂PO₄⁻ was adsorbed more strongly than SiO₃²⁻ on synthetic iron oxides and oxyhydroxides [41]. As a result, H₂PO₄⁻ showed more negative effect on TC removal than SiO₃²⁻. These results were informative for in situ remediation using NZVI due to the coexistence of competitive anions in natural environment.

3.2.8. Analysis of degradation products

As an electron donor, NZVI is effective in the transformation of a wide array of common environmental contaminants such as chlorinated solvents, heavy metal ions and organic dyes [17,37,42,43] due to its strong reduction characteristics. Experiments were performed to detect the byproducts of TC using LC-ESI-MS after treatment by PVP-NZVI. Fig. 8 presents the LC-MS spectra of TC, supernatant samples (pH 3.0 and 6.5) and the dissolved sample. The data of mass spectrum of these samples were similar, revealing that the degradation products adsorbed on the surface of PVP-NZVI were the same as the degradation products in treated solution. In other words, PVP-NZVI can adsorb not only TC but also the degradation products. At the retention time of 2.1 min, TC molecular was eluted. After reaction for 4 h at initial pH of 3.0 and 6.5, a new flow peak was observed at retention time of 1.8 min. Three anions with *m/z* of 270.8, 329.6 and 387.1 were identified and the anion with *m/z* of 444.9 is designated to TC molecule. These observations suggest that the main intermediates with *m/z* of 270.8, 329.6 and 387.1 are generated during reaction. Based on LC-MS results, the main degradation products of TC by PVP-NZVI are proposed in Table 3. Product 1 (*m/z* 387.1) is originated from TC degradation via loss of N-methyl and amino group due to the low bond energy of N–C [44] and the loss of hydroxyl group [45]. Further degradation of Product 1 (*m/z* 387.1) leads to the generation of Product 2 (*m/z* 329.6) via the loss of amino group and hydroxyl group [46]. Then degradation of Product 2 (*m/z* 329.6) leads to the generation of Product 3 (*m/z* 270.8) via the loss of carbonyl group and formyl group.

**Fig. 9.** Proposed reduction cleavage of TC and three main degradation products.

LC-MS analysis shows that the main degradation products were resulted from TC after the losses of some groups from the ring. Fig. 9 shows the fragmentation pattern suggested for TC. Principal fragmentations probably resulted from loss of water, ammonia,

dimethylamino group, carbonyl and hydroxyl. The degradation TC was mainly transformed into the products with similar structures to TC.

4. Conclusions

The present study demonstrated that the PVP-K30 modified NZVI can be used as an effective and low-cost material for the effective removal of TC in wastewater. The performance of batch experiments under various conditions indicated that PVP-NZVI had superior removal ability toward TC over the range of 50.0–300.0 mg/L. pH is a significant factor affecting the removal efficiency of TC by PVP-NZVI. The removal of TC is more effective in acidic and neutral pH. The inner-sphere complex-forming anions phosphate, silicate, competed strongly with TC for sorption sites, whereas sulfate and acetate only inhibited the removal of TC slightly. The removal capacity increased as temperature increased. LC–MS analysis showed that the degradation products were mainly stemmed from TC after the losses of some groups from the ring. The data of MS spectra indicated that PVP-NZVI can adsorb not only TC but also the degradation products. Additional investigations are necessary to verify whether the degradation products of TC could pose serious environmental risks.

Acknowledgement

The authors would like to thank the National Natural Science Foundation of China (40973074) for financial support of the present study.

References

- [1] S. Sassman, L. Lee, Sorption of three tetracyclines by several soils: assessing the role of pH and cation exchange, *Environ. Sci. Technol.* 39 (2005) 7452.
- [2] A.K. Sarmah, M.T. Meyer, A.B.A. Boxall, A global perspective in the use, sales, exposure pathways, occurrence, fate and effects of veterinary antibiotics (VAs) in the environment, *Chemosphere* 65 (2006) 725–759.
- [3] W. Ben, Z. Qiang, C. Adams, H. Zhang, L. Chen, Simultaneous determination of sulfonamides, tetracyclines and tiamulin in swine wastewater by solid-phase extraction and liquid chromatography–mass spectrometry, *J. Chromatogr. A* 1202 (2008) 173–180.
- [4] S.Q. Zhang, Analysis of harmful components and harmless processing of livestock and poultry manures from feedlots, Report for Postdoctoral research, Chinese Academy of Agricultural Sciences, Beijing, 2004.
- [5] H.T. Pawelzick, H. Höper, H. Nau, G. Hamscher, A survey of the occurrence of various tetracyclines and sulfamethazine in sandy soils in northwestern Germany fertilized with liquid manure, in: SETAC Euro 14th Annual Meeting, Prague, Czech Republic, April 18–22, 2004.
- [6] Animal Health Institute, 1997 Market Research Report, U.S. Animal Health Product Industry: Alexandria, VA, 1997, p. 59.
- [7] M.E. Lindsey, M. Meyer, E.M. Thurman, Analysis of trace levels of sulfonamide and tetracycline antimicrobials in ground-water and surface water using solid-phase extraction and liquid chromatography/mass spectrometry, *Anal. Chem.* 73 (2001) 4640–4646.
- [8] G. Hamscher, S. Sczesny, H. Hoepfer, H. Nau, Determination of persistent tetracycline residues in soil fertilized with liquid manure by high-performance liquid chromatography with electrospray ionization tandem mass spectrometry, *Anal. Chem.* 74 (2002) 1509–1518.
- [9] J. Zhu, D.D. Snow, D.A. Cassada, S.J. Monson, R.F. Spalding, Analysis of oxytetracycline, tetracycline, and chlortetracycline in water using solid-phase extraction and liquid chromatography–tandem mass spectrometry, *J. Chromatogr. A* 928 (2001) 177–186.
- [10] M. De Liguoro, V. Cibin, F. Capolongo, B.H. Sørensen, C. Montesissa, Use of oxytetracycline and tylosin in intensive calf farming: evaluation of transfer to manure and soil, *Chemosphere* 52 (2003) 203–212.
- [11] F. He, D. Zhao, Manipulating the size and dispersibility of zerovalent iron nanoparticles by use of carboxymethyl cellulose stabilizers, *Environ. Sci. Technol.* 41 (2007) 6216–6221.
- [12] Y. Sun, X. Li, J. Cao, W. Zhang, H. Paul Wang, Characterization of zero-valent iron nanoparticles, *Adv. Colloid Interface Sci.* 120 (2006) 47–56.
- [13] S.R. Kanel, J.M. Grenche, H. Choi, Arsenic(V) removal from groundwater using nano scale zero-valent iron as a colloidal reactive barrier material, *Environ. Sci. Technol.* 40 (2006) 2045–2050.
- [14] A.B.M. Giasuddin, S.R. Kanel, H. Choi, Adsorption of humic acid onto nanoscale zerovalent iron and its effect on arsenic removal, *Environ. Sci. Technol.* 41 (2007) 2022–2027.
- [15] L.J. Kecskes, R. Woodman, S.F. Trevino, B.R. Klotz, S.G. Hirsch, B.L. Gersten, Characterization of a nanosized iron powder by comparative methods, *Kona* 21 (2003) 143–150.
- [16] Y. Sun, X. Li, W. Zhang, H. Paul Wang, A method for the preparation of stable dispersion of zero-valent iron nanoparticles, *Colloids Surf. A: Physicochem. Eng. A* 308 (2007) 60–66.
- [17] D. Karabelli, C. Uzum, T. Shalhwan, A.E. Eroglu, T.B. Scott, K.R. Hallam, I. Lieberwirth, Batch removal of aqueous Cu²⁺ ions using nanoparticles of zero-valent iron: a study of the capacity and mechanism of uptake, *Ind. Eng. Chem. Res.* 47 (2008) 4758–4764.
- [18] M. Alowitz, M. Scherer, Kinetics of nitrate, nitrite, and Cr (VI) reduction by iron metal, *Environ. Sci. Technol.* 36 (2002) 299–306.
- [19] G. Naja, A. Halasz, T. Sonia, A. Guy, H. Jalal, Degradation of hexahydro-1,3,5-trinitro-1,3,5-triazine (RDX) using zerovalent iron nanoparticles, *Environ. Sci. Technol.* 42 (2008) 4364–4370.
- [20] B.L. Cushing, V.L. Kolesnichenko, C.J. O'Connor, Recent advances in the liquid-phase syntheses of inorganic nanoparticles, *Chem. Rev.* 104 (2004) 3893–3946.
- [21] F. He, D. Zhao, Preparation and characterization of a new class of starch-stabilized bimetallic nanoparticles for degradation of chlorinated hydrocarbons in water, *Environ. Sci. Technol.* 39 (2005) 3314–3320.
- [22] L. Guo, S. Yang, C. Yang, P. Yu, J. Wang, W. Ge, K. George, L. Wong, Synthesis and characterization of poly(vinylpyrrolidone)-modified zinc oxide nanoparticles, *Chem. Mater.* 12 (2000) 2268–2274.
- [23] A. El Badawy, T. Luxton, R.G. Silva, K.G. Scheckel, M.T. Suidan, T.M. Tolaymat, Impact of environmental conditions (pH, ionic strength, and electrolyte type) on the surface charge and aggregation of silver nanoparticles suspensions, *Environ. Sci. Technol.* 44 (2010) 1260–1266.
- [24] C. Gu, K.G. Karthikeyan, Interaction of tetracycline with aluminum and iron hydrous oxides, *Environ. Sci. Technol.* 39 (2005) 2660–2667.
- [25] K.F. Rubert, J.A. Pedersen, Kinetics of oxytetracycline reaction with a hydrous manganese oxide, *Environ. Sci. Technol.* 40 (2006) 7216.
- [26] K.J. Choi, S.G. Kim, S.H. Kim, Removal of tetracycline and sulfonamide classes of antibiotic compound by powdered activated carbon, *Environ. Technol.* 29 (2008) 333–342.
- [27] P.H. Chang, Z. Li, T.L. Yu, S. Munkhbayer, T.H. Kuo, Y. Hung, J.S. Jean, K.H. Lin, Sorptive removal of tetracycline from water by palygorskite, *J. Hazard. Mater.* 165 (2009) 148–155.
- [28] R.A. Figueroa, A.A. MacKay, Sorption of oxytetracycline to iron oxides and iron oxide-rich soils, *Environ. Sci. Technol.* 39 (2005) 6664–6671.
- [29] C. Wang, W. Zhang, Synthesizing nanoscale iron particles for rapid and complete dechlorination of TCE and PCBs, *Environ. Sci. Technol.* 31 (1997) 2154–2156.
- [30] J. Sokol, E. Matisova, Determination of tetracycline antibiotics in animal tissues of food-producing animals by high-performance liquid chromatography using solid-phase extraction* 1, *J. Chromatogr. A* 669 (1994) 75–80.
- [31] X. Li, W. Zhang, Iron nanoparticles: the core-shell structure and unique properties for Ni(II) sequestration, *Langmuir* 22 (2006) 4638–4642.
- [32] Y. Liu, H. Choi, D. Dionysiou, G.V. Lowry, Trichloroethene hydrodechlorination in water by highly disordered monometallic nanoiron, *Chem. Mater.* 17 (2005) 5315–5322.
- [33] J.T. Nurmi, P.G. Tratnyek, V. Sarathy, D.R. Bae, J.E. Amonette, K. Peche, C. Wang, J.C. Linehan, D.W. Matson, R. Leppenn, M.D. Driessen, Characterization and properties of metallic iron nanoparticles: spectroscopy, electrochemistry, and kinetics, *Environ. Sci. Technol.* 39 (2005) 1221–1230.
- [34] S. Goldberg, C.T.J. Johnston, Mechanisms of arsenic adsorption on amorphous oxides evaluated using macroscopic measurements, vibrational spectroscopy, and surface complexation modeling, *J. Colloid Interface Sci.* 234 (2001) 204–216.
- [35] J.M. Wessels, W.E. Ford, W. Szymczak, S. Schneider, The complexation of tetracycline and anhydrotetracycline with Mg²⁺ and Ca²⁺: a spectroscopic study, *J. Phys. Chem. B* 102 (1998) 9323–9331.
- [36] C.F. Baes Jr., R.E. Mesmer, *The Hydrolysis of Cations*, Wiley, New York, 1976, pp. 489.
- [37] C. Su, R.W. Puls, Arsenate and arsenite removal by zerovalent iron: kinetics, redox transformation, and implications for in situ groundwater remediation, *Environ. Sci. Technol.* 35 (2001) 1487–1492.
- [38] K. Rubert, J.A. Pedersen, Kinetics of oxytetracycline reaction with a hydrous manganese oxide, *Environ. Sci. Technol.* 40 (2006) 7216.
- [39] D. Burris, T. Campbell, C. Valipuram, S. Manoranjan, Sorption of trichloroethylene and tetrachloroethylene in a batch reactive metallic iron–water system, *Environ. Sci. Technol.* 29 (1995) 2850–2855.
- [40] C. Appelo, M. Weiden, C. Tournasat, L. Charlet, Surface complexation of ferrous iron and carbonate on ferrihydrite and the mobilization of arsenic, *Environ. Sci. Technol.* 36 (2002) 3096–3103.
- [41] X. Meng, G. Korfiatis, S. Bang, K.W. Bang, Combined effects of anions on arsenic removal by iron hydroxides, *Toxicol. Lett.* 133 (2002) 103–111.
- [42] Z. Zhang, N. Cissoko, J. Wo, X. Xu, Factors influencing the dechlorination of 2,4-dichlorophenol by Ni–Fe nanoparticles in the presence of humic acid, *J. Hazard. Mater.* 165 (2009) 78–86.
- [43] W. Zhang, C. Wang, H. Lien, Treatment of chlorinated organic contaminants with nanoscale bimetallic particles, *Catal. Today* 40 (1998) 387–395.
- [44] D. Raphael, D. Maume, B.L. Bizet, H. Pouliquen, Preliminary assays to elucidate the structure of oxytetracycline's degradation products in sedi-

- ments, determination of natural tetracyclines by high-performance liquid chromatography–fast atom bombardment mass spectrometry, *J. Chromatogr. B* 748 (2000) 369–381.
- [45] I. Dalmázio, M. Almeida, R. Augusti, T.M.A. Alves, Monitoring the degradation of tetracycline by ozone in aqueous medium via atmospheric pressure ionization mass spectrometry, *J. Am. Soc. Mass Spectrom.* 18 (2007) 679–687.
- [46] S. Jiao, S. Zheng, D. Yin, L. Wang, L. Chen, Aqueous photolysis of tetracycline and toxicity of photolytic products to luminescent bacteria, *Chemosphere* 73 (2008) 377–382.
- [47] M.F.M. Tavares, V.L. McGuffin, Separation and characterization of tetracycline antibiotics by capillary electrophoresis, *J. Chromatogr. A* 686 (1994) 129–142.